Polymerization of Carbon Nanotubes through Self-Irradiation

Rodrigo Link Federizzi,[†] Cássio Stein Moura,*[,‡] and Livio Amaral[†,‡]

Material Science Program, Institute of Physics, Universidade Federal do Rio Grande do Sul, C.P.: 15051, 91501−070 Porto Alegre, RS, Brazil

Received: July 31, 2006; In Final Form: September 14, 2006

We have investigated the formation of cross-links between neighboring carbon nanotubes within a bundle. Classical molecular dynamics was used to follow the evolution of the system when it is bombarded by low-energy carbon atoms. We show that it is possible to polymerize carbon nanotubes through irradiation and discuss the most common types of defects produced. Cross-links are created mainly in the direction perpendicular to the surface, and for higher energies, defects are created deeper in the rope. The final defects geometries may provide a realistic input to electronic density first principle calculations.

1. Introduction

Among the not so far potential applications that have been proposed for carbon nanotubes (CNTs) is the possibility of building up super-tough fibers. Such fibers can be weaved to make very strong cables or textiles. Even a space elevator made of CNTs has been proposed.[1] Long CNT bundles have been generated by several research groups. Zhu[2] has synthesized long strands of ordered single-walled carbon nanotubes (SWCNTs) by catalytic chemical vapor deposition. Their rope lengths range between 10 and 20 cm. Dalton et al.[3] used a coagulation-based process that yields a 100-m-long yarn made of SWCNTs at a reasonable rate for industrial production. The tensile strength of such fiber reaches 1.8 GPa, and the energy absorption is more than 10 times the value presented by Kevlar fiber. Such impact damping is significant for bullet-proof vests. Similar values were reported by Miaudet et al.[4] that employed a hot-drawing process. Such CNT fibers have tensile strength higher than spider silk (1.5 GPa [5]) and a density smaller than steel.

A single CNT has a tensile strength larger than a rope made of several SWCNTs. Li et al.[6] have performed mechanical tests to compare both cases. Whereas a SWCNT presented a tensile strength of up to 22.2 GPa, threads made of several CNTs had tensile strengths ranging from 2.3 to 14.2 GPa. Such a difference in strength is due to the weak van der Waals interaction between neighboring tubes compared to the strong covalent bonding between atoms in the same tube. When a single tube is pulled, it may simply slip over its neighbors, decreasing the strength of the fiber. To avoid such slippage and increase the bundle strength, it is necessary to create strong chemical bonding between adjacent tubes. Despite the fact that spontaneous polymerization has been foreseen theoretically,[7] several approaches have been proposed to force it to happen as we describe next.

Chemical functionalization has shown to be an effective way of producing cross-links. Ni et al.[8] have shot CF_3^+ ions at incident energies below 100 eV and examined the nanotubes with X-ray photoelectron spectroscopy and scanning electron microscopy. Their results indicate that the tubes were functionalized and connections between the tubes were formed.

Defects could also provide the necessary conditions for intertube connections. CNTs are known as a quasi-perfect lattice having a very small amount of defects. Electrochemical methods showed that SWCNTs can have a defect concentration as low as 4 μm^{-1}.[9,10]

Kis et al.[11] have irradiated CNT bundles with medium energy electrons and observed a 30-fold increase in the bending modulus of the irradiated ropes compared to the virgin samples. Above 86 keV, defect production overcomes cross-linking production, turning the process less effective. Moreover, they suggest that cross-linking through functional groups, like carboxyl or hydroxyl, is much less probable than through interstitial carbon atoms generated during irradiation. Following these results, Da Silva and collaborators[12] performed ab initio calculations and showed that Frenkel pairs, which have a low formation energy, are very likely to be produced during irradiation and could play an important role on cross-links formation. Moreover, Sammalkorpi et al.[13] have shown through molecular dynamics simulations (MD) that, besides the fact that defects can lead to cross-link formation and further increase in mechanical strength, vacancies alone do not affect significantly Young modulus though the tensile strength drops significantly in the presence of single vacancies. It would be necessary to have a very high concentration, above 50 $Å^{-1}$, to notice any effect. However, Zhang et al.[14] report a decrease on the range of 20−33% on the fracture strength due to the presence of single and double vacancies. Basiuk et al.[15] irradiated SWCNTs with high-energy protons and observed that for doses higher than 1 mC, samples degrade into amorphous material.

Application of pressure on CNT samples can lead to polymerization as well. Popov et al.[16] applied pressures up to 55 GPa to SWCNT samples and observed an increase in the bulk modulus of up to 546 GPa. Those authors obtained Raman spectra that suggest that the increase in hardness is due to irreversible changes in the CNT structure, which were associated with cross-linkage in the sample. High-temperature treatment applied concurrently to pressure seems to lead to similar results, as discussed by Khabashesku et al.[17] In addition, polymerization under pressure at room temperature has been reported for C_{60}.[18] A recent paper[19] shows MD simulations of applied pressure on

* To whom correspondence should be addressed. E-mail: cmoura@if.ufrgs.br; Phone: +55 51 33167250; Fax: +55 51 33167286.
† Institute of Physics.
‡ Material Science Program.

10.1021/jp064907g CCC: $33.50
Published on Web 10/25/2006

CNTs and claims that extensive polymerization at room temperature is only possible for small diameter tubes, namely, 5 Å.

Several groups have simulated irradiation of CNTs to describe defect formation and their consequences. Most works deal with noble-gases irradiation on CNTs.[20−23] Nonetheless, some works report simulations of other projectile species as electrons and fluorocarbon ions,[24] potassium,[25] boron, and nitrogen,[26] which have important applications on electronics. First principles calculations have been used to study the electronic structure and bond configurations due to adsorption in CNTs.[27−29] Nevertheless, those kind of calculations need as input the position of the adsorbed atom with respect to the tube surface. Experiments, like the one done by Kis et al.,[11] cannot determine such geometry and first-principles approaches employ a hypothetical force on a carbon atom to simulate vacancy formation. Therefore, MD calculations stand midway between both approaches for the adatom position is an output of the irradiation simulations.

Besides mechanical effects derived from ion irradiation, some electronic and transport properties have been studied. Although one-dimensional metallic SWCNT is not expected to fall into the strong localization regime, there are evidences for a weak localization diffusive regime and quantum interference in multiwall CNTs.[30] Gómez-Navarro et al.[31] showed that it is possible to tune SWCNT conductance through ion irradiation. The authors performed simulations employing a first principles local orbital density-functional method and claim that an insight about vacancies-like defects is important for the rationale behind the observation of the strong localization regime.

In this work, we have performed MD simulations of carbon irradiation on bundles of SWCNTs. Because our goal is to improve mechanical strength of such a system, we decided to choose carbon as the projectile to avoid introducing extra impurities. With respect to defect creation, two things may happen to the incoming projectile: either it becomes part of the final defect configuration or it undergoes a replacement collision and the displaced atom may take part on the defect. In the last case rests the main advantage of performing self-irradiation: the substitutional atom does not become an extra impurity.

2. Computational Details

Our simulation code performs classical molecular dynamics employing Tersoff[32] potential in order to describe carbon−carbon interactions at near-equilibrium atomic distances. At small distances, Tersoff potential gives an incorrect description of the interaction. Therefore, for small distances, the universal ZBL potential[33] is used. The ZBL potential is composed by a coulomb term and a screening function:

$$U_{\mathrm{ZBL}}(r_{ij}) = \frac{Z_i Z_j}{r_{ij}}\phi(r_{ij}) \tag{1}$$

where Z_i and Z_j are the atomic numbers of particles i and j, and r_{ij} is the interatomic distance. The screening function $\phi(r_{ij})$ is given by:

$$\phi(r_{ij}) = \sum_{l=1}^{4} b_l \exp\left[c_l \frac{r_{ij}}{a}\right] \tag{2}$$

where a is a reduced distance and b_l and c_l are parameters whose values can be found in ref 33. To ensure a smooth transition between both potentials, e.g., continuous function and its first derivative, we define a bridging potential, which modulates the other two potentials:

$$U_{\mathrm{bridge}}(r_{ij}) = \exp[-r_{ij}^2]U_{\mathrm{ZBL}}(r_{ij}) + 0.9\exp[-(r_{ij}-0.325)^2]U_{\mathrm{Tersoff}}(r_{ij}) \tag{3}$$

This potential is turned on for distances smaller than 0.545 Å. It has already been used to simulate channeling in CNTs.[34,35]

The CNT bundle is composed of nine (10,10) SWCNT separated by a distance of 3.2 Å. Each tube has 1000 atoms and periodic boundary conditions are used along the longitudinal direction in order to mimic an infinitely long strand. Figure 1 depicts the system initial configuration. An extra carbon atom is placed near an outer tube at a distance larger than the potential cutoff radius and receives a certain velocity perpendicular to the bundle longitudinal axis. To have good statistics, for each incidence energy, the projectile was systematically shot 460 times scanning an area of 2 × 10 Å. Each simulation starts with a fresh sample. We have chosen to simulate four incident energies: 50, 100, 150, and 200 eV. Temperature was kept fixed at 300 K using Andersen thermostat.[36] The time step was set to 0.1 fs to have good energy conservation. The simulation stops when all particle motion is due only to thermal random motion.

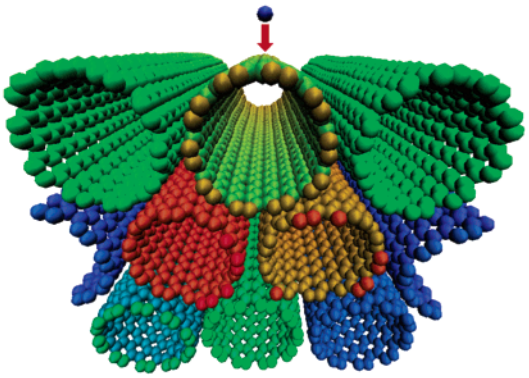

Figure 1. Initial configuration of a CNT bundle irradiation. The extra atom receives a momentum perpendicular to the bundle surface. Periodic boundary conditions were applied on the left-right directions and on the direction perpendicular to the page. The top-bottom boundary was kept free.

3. Results and Discussion

The collision of the external atom with the CNT bundle may cause the production of cross-links or not. Let us analyze first the case when cross-links are not formed but only simple defects. Figure 2 shows the atomic positions of the seven most common configurations (which will be called defects hereafter) that we have observed in our simulations. Table 1 summarizes the bond-length and angles that characterize each kind of defect, which will be detailed below.

The most common defect is the single internal adsorption. In such a defect, an extra atom becomes trapped inside a CNT and bonds internally to one atom of the surface. We consider that a bond exists when two atoms stay closer than 1.7 Å. It is created with a probability of 48% at 50 eV, soaring up to 61% at 200 eV, as shown in Figure 3. The defect creation probability was calculated as follows. For each shot, we observe if at least one defect of that kind is formed. Duplicated defects count as one, which means that we are considering the probability of defect creation and not the absolute number of defects. After all runs, the number of times defects were created is divided by 460, the total number of runs for each energy.

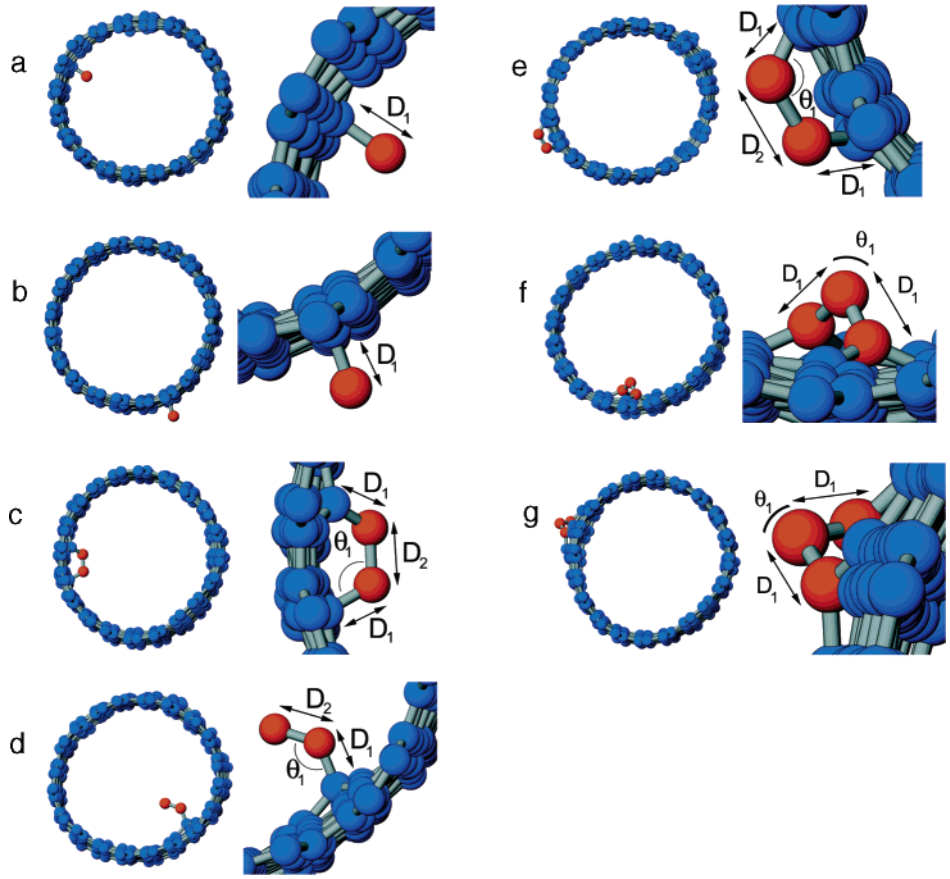

Figure 2. (a) Configuration of a single internal adsorption. (b) Configuration of a single external adsorption. (c) Configuration of a double n-internal adsorption. (d) Configuration of a double L-internal adsorption. (e) Configuration of a double n-external adsorption. (f) Configuration of a triple internal adsorption. (g) Configuration of a triple external adsorption.

TABLE 1: Defects Parameters for Simple Defects on a CNT Rope

	D_1 (Å)	D_2 (Å)	angle (deg)
single internal adsorption	1.46 ± 0.06	-	-
single external adsorption	1.43 ± 0.04	-	-
triple internal adsorption	1.38 ± 0.05	-	109.9 ± 6.9
triple external adsorption	1.37 ± 0.04	-	114.9 ± 6.2
double L-internal adsorption	1.46 ± 0.06	-	123.8 ± 2.7
double n-internal adsorption	1.45 ± 0.07	1.46 ± 0.06	124.3 ± 3.8
double n-external adsorption	1.43 ± 0.05	1.41 ± 0.04	122.4 ± 2.9

Another common defect is the single external adsorption. In this kind of defect, which resembles the internal adsorption, an extra atom gets adsorbed onto the external tube surface and bonds to only one tube. There is no cross-link creation in this kind of defect. However, we believe that a further thermal treatment could bring those adatoms to places where bonding between neighboring tubes could be formed. Figure 3 shows that the probability of creating a single external adsorption becomes larger when the energy increases. Therefore, formation of such defect is advantageous for it could cooperate on cross-link formation. Our results are in line with the work of Ni et al.[8] who have irradiated bundles of SWCNTs with CH_3 projectiles. At an incidence energy of 80 eV, they found a probability of 36% of atoms and fragments getting adsorbed on the surface. For a similar energy, e.g., 100 eV, we found a probability of 44% of external adsorption. A CH_3 ion has three saturated bonds and only one dangling bond whereas a single C atom has all four valence electrons able to build up bonds with the surface atoms. We believe this could be the reason a C atom has a higher probability of getting adsorbed than the CH_3 ion or its fragments that have less than four dangling bonds.

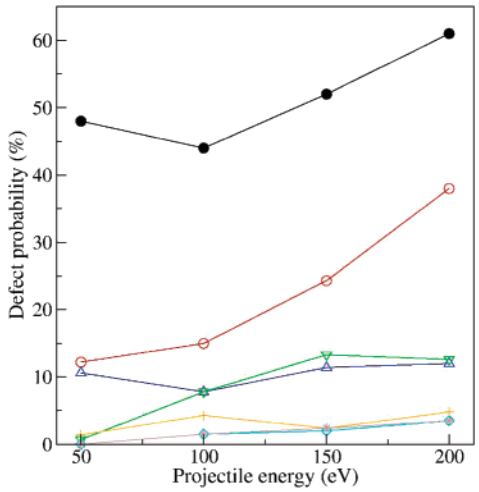

Figure 3. Probability of creating defects with no cross-links. Key of symbols: single internal adsorption: -●-; single external adsorption: -○-; triple internal adsorption: -△-; triple external adsorption: -▽-; double L-internal adsorption: -+-;double n-internal adsorption: -◇-; double n-external adsorption: -∗-. Lines were drawn only to guide the eyes.

With a reasonable occurrence probability, we observe the creation of a sort of defect containing three atoms forming a triangle either internal or external to the nanotube. The formation probability of such defect within the nanotube seems to be independent of projectile energy, as shown by the blue line in Figure 3. On the other hand, the external triangle is very rare at 50 eV but increases its probability, saturating at around 13% for the energy range that we have studied.

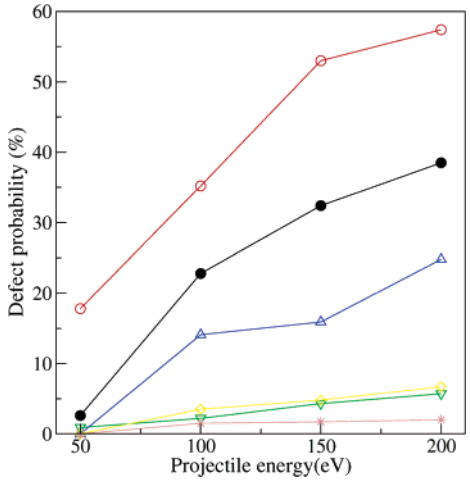

Figure 4. Probability of creating defects with cross-links. Key of symbols: single-atom cross-link: -○-; direct cross-link: -●-; triangle cross-link: -△-; h-cross-link: -◇-; double-atom cross-link: -▽-; H-cross-link: -∗-. Lines were drawn only to guide the eyes.

When two atoms become adsorbed closely to each other, different defects may be formed. If both atoms bond to the nanotube, they form a half hexagon together with the tube atoms. This kind of double adsorption may happen either internally or externally to the tubes. When only one atom bonds to the surface and the other one stays in a dangling position, we call it a L-adsorption. This kind of defect usually occurs internally to the nanotube. The external version of the L-adsorption is so rare that we did not plot it in Figure 3. Similarly, other kinds of defects that were also very rare to happen were not considered in this paper.

Cross-links may be produced with a high probability as shown by Figure 4. The most common case of cross-linking happens when an extra atom sits between two neighboring tubes. Figure 5 shows the cross-links geometries. When such configuration happens, the interaction between tubes may change from weak van der Waals to strong covalent bonding. It is expected that this connection may increase the mechanical strength of a CNT bundle. One can observe in Figure 4 that the creation probability increases linearly up to 150 eV, increasing more slowly after this point. The geometrical parameters for the observed cross-links are given in Table 2. It is worth saying that the values given in Tables 1 and 2 are the averages over the whole energy range.

The collisional process may create waves in the nanotube surface, as discussed by us in ref 35. When the wave amplitude becomes large, neighboring tubes may become closer and get connected through a direct connection. We considered that such a direct cross-link happens every time two atoms pertaining to different tubes stay closer than 1.7 Å. This is the second most common cross-link that we have observed. It quickly increases its creation probability for low projectile energies but grows in a smaller rate for energies beyond 100 eV.

The third most common cross-link to happen is the one we call triangle defect. In this case, the extra atom bonds to only one atom in one tube and bonds to two atoms in the other tube. The main difference to the most common cross-link discussed above is that, in that case, the extra atom bonds to only two atoms, one at each tube. Once more, we can observe in Figure 4 an increase in the creation probability for higher energies.

There are other kinds of possible cross-link that are listed in Table 2 and Figure 5, namely, 2-atom cross-link, h-cross-link, and H-cross-link. All of them have low creation probability. However, their creation probability shows a slow growth with projectile energy. Ni et al.[8] have reported a defect similar to the one we labeled H-cross-link. However, they have observed that defect between two shells of the same double-wall CNT.

Observing Figures 3 and 4, one may notice that although the probability of cross-linking always increases with energy, the same behavior does not happen for defect creation. Excepting single adsorption, either internal or external, all kinds of defects tend to reach a stable production rate. Single internal adsorption reaches a probability of 61% at 200 eV. This kind of defect does not alter significantly the structure of the SWCNTs, for in most cases the extra atom within the tube comes from a substitutional collision. The projectile replaces the atom at which it impinges at first, keeping the local structure unaltered, while the ejected atom becomes attached to the internal surface. We observed that substitutional collisions happened in 54% of overall simulations. In the case of multiwall carbon nanotubes (MWCNT), this kind of defect becomes important, for it may provide cross-links between the tube layers, as discussed by Pregler.[24] In a similar way, single external adsorption tends to increase its creation probability, reaching 38% at 200 eV. If a postirradiation thermal annealing was applied to the system, the adsorbed atom could reach a region close enough to neighboring tubes and become a cross-link. Therefore, such defect is desirable for cross-linking. We may conclude that self-irradiation is a good choice in order to generate CNT polymerization.

We did not investigate higher energies because it would need a larger system and, consequently, a more powerful computational facility. Up to 150 eV, particle transmission through our three-layer bundle happened with a probability lower than 1%, being 0% for 50 eV. However, for 200 eV, the probability increased up to 6%. Some particles leaving the last CNT layer presented energy of up to 56 eV. Nevertheless, cross-linking happens mainly at the surface, even for an energy of 200 eV, as it will be discussed next.

Figure 6 shows the amount of cross-links formed between the bundle layers for each projectile energy. Label 1−1 represents the number of cross-links formed between two tubes on the first layer of the surface; label 1−2 means the number of cross-links formed between a tube on the first layer and a tube on the second layer; etc. As one can observe, cross-linking is favored by an increase in the energy. Moreover, higher energies create cross-links deeper in the bundle. Analyzing Figure 6, one can conclude that linking of tubes in the same layer happens less frequently than linking tubes in different layers. This is very convenient, for in order to build a stronger CNT fiber, it is more advantageous to create links between different layers. The reason that happens is because the

TABLE 2: Defects Parameters for Crosslinks on a CNT Rope

	D_1 (Å)	D_2 (Å)	D_3 (Å)	angle (deg)	angle (deg)
direct cross-link	1.44 ± 0.04	-	–	–	–
1-atom cross-link	1.46 ± 0.05	-	–	127.9 ± 5.0	–
2-atom cross-link	1.45 ± 0.05	1.48 ± 0.03	–	124.7 ± 3.2	–
triangle cross-link	1.39 ± 0.06	1.44 ± 0.04	–	110.7 ± 5.3	–
h-cross-link	1.43 ± 0.05	1.42 ± 0.05	1.46 ± 0.05	115.5 ± 6.6	119.5 ± 5.4
H-cross-link	1.45 ± 0.05	1.42 ± 0.04	–	120.7 ± 4.7	–

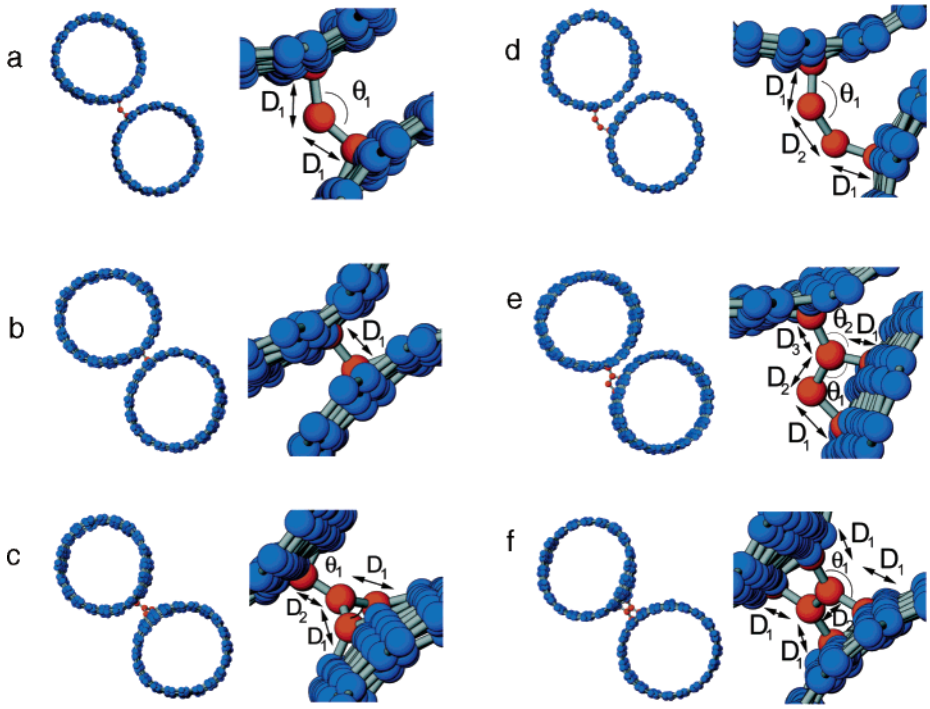

Figure 5. (a) Single-atom cross-link. (b) Direct cross-link. (c) Triangle cross-link. (d) Double-atom cross-link. (e) h- cross-link. (f) H-cross-link.

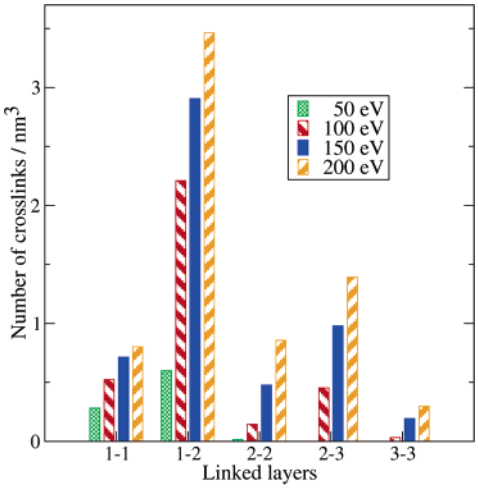

Figure 6. Number of cross-links formed between layers normalized by the volume of the bundle.

momentum of the impinging carbon atoms is much higher at directions joining different layers, turning the cross-link more probable at this direction. Observing the projectile trajectory, we have seen that when the projectile reaches the rope surface, it may get into the groove between the outermost tubes, going straight to the second layer. When it reaches that layer, the projectile deviates sideways and may become a cross-link between the first and second layer. In a similar way, the projectile may go through a tube in the external layer and reach the groove between the tubes in the second layer, being scattered on the third layer. At that point it could produce a cross-link between the second and third layer.

On the other hand, Figure 6 shows that it is quite unlike creating cross-links beyond the third surface layer, at least for the low energy limit considered in this work. It is worth saying that the lack of a fourth layer, which could backscatter particles to form links within 3−3 and 3−4 layers, ends up underestimating the formation probability of such cross-links. However, this error must be roughly 6%, the transmission probability, for 200 eV projectiles.

Our results are in concordance with the work of Salonen et al.[20] who have performed simulations of Ar irradiation of bundles of CNTs and found some of the defects reported here. However, they did not describe in more details those defects. They have shown that most defects are produced in the interface region within adjacent nanotubes. For projectiles at the same energy range as this work, they observed defect formation only within the first two layers of the sample. Despite the fact that argon is heavier than carbon they observed that, for a 500 eV projectile, only a small amount of defects was produced beyond the third layer. Therefore, one can say that for low energy atoms, only the external layers of the sample may get polymerized.

Backscattering showed to be a non-negligible effect. For the energies of 50, 100, 150, and 200 eV, the projectile returned with the following probabilities, respectively: 3, 5, 7, and 11%.

4. Summary

In this work, we have performed molecular dynamics simulations of a low-energy atom being shot against a 3-layer carbon nanotube rope. We have observed the formation of several kinds of defects including cross-links between the tubes that could be used to increase the mechanical strength of CNT ropes. Such improvement has been observed experimentally. However, experimental techniques are not able to tell where and which kind of defects are created. Our simulations provide the geometry of those defects that could be used as a more realistic input data for electronic structure calculations based on first principles approaches.

We observed that the most common defect is the single adsorption, which can happen either internally or externally to the tube. Cross-linking is also very likely to occur, the most common type being the one in which a single particle sits between two tubes and bonds to them. The change from van der Waals interaction to covalent bonding between the tubes is expected to increase the mechanical strength of the CNT rope.

More energetic projectiles seem to increase the number of defects and intertube cross-linking, as well as creating them

deeper in the fiber. However, for some defects, after a certain threshold, damage formation increases in a slower rate whereas cross-link formation seems to keep increasing. The kind of defects that keep increasing the creation probability when the projectile energy increases, e.g., single internal/external adsorption, either do not contribute to the bundle fragilization or may help cross-link formation. Therefore, we may affirm that self-irradiation is an advantageous way of polymerizing ropes made of single-wall carbon nanotubes. Meanwhile, we observed that cross-links have a higher probability to take place in the direction perpendicular to the rope surface than between tubes in the same depth. This finding is quite valuable, for if bonding happened primarily between tubes in the same layers, then external tubes would be able to slip over internal layers, which is undesirable.

Acknowledgment. We acknowledge the Brazilian funding agencies CNPq and CAPES for their financial support.

References and Notes

(1) Edwards, B. C. *Acta Astron.* **2000**, *47*, 735.
(2) Zhu, H. W.; Xu, C. L.; Wu, D. H.; Weil, B. Q.; Vajtai, R.; Ajayan, P. M. *Science* **2002**, *296*, 884.
(3) Dalton, A. B.; Collins, S.; Muñoz, E.; Razal, J. M.; Ebron, V. H.; Ferraris, J. P.; Coleman, J. N.; Kim, B. G.; Baughman, R. H. *Nature (London)* **2003**, *423*, 703.
(4) Miaudet, P.; Badaire, S.; Maugey, M.; Derré, A.; Pichot, V.; Launois, P.; Poulin, P.; Zakri, C. *Nano Lett.* **2005**, *5*, 2212.
(5) Griffiths, J. R.; Salanitri, V. R. *J. Mater. Sci.* **1980**, *15*, 491.
(6) Li, F.; Cheng, H. M.; Bai, S.; Su, G.; Dresselhaus M. S. *App. Phys. Lett.* **2000**, *77*, 3161.
(7) Cheng, H.; Pez, G. P.; Cooper, A. C. *Nano Lett*. **2003**, *3*, 585.
(8) Ni, B.; Andrews, R.; Jacques, D.; Qian, D.; Wijesundara, M. B. J.; Choi, Y.; Hanley, L.; Sinnott; S. B. *J. Phys. Chem.* **2001**, *105*, 12719.
(9) Fan, Y.; Goldsmith, B. R.; Collins, P. G. *Nat. Mater.* **2005**, *4*, 906.
(10) Ebbesen, T. W.; Takada, T. *Carbon* **1995**, *33*, 973.
(11) Kis, A.; Csányi, G.; Salvetat, J.-P.; Lee, T.-N.; Couteau, E.; Kulik, A. J.; Benoit, W.; Brugger, J.; Forró, L. *Nat. Mater.* **2004**, *3*, 153.
(12) Da Silva, A. J. R.; Fazzio, A.; Antonelli, A. *Nano Lett.* **2005**, *5*, 1045.
(13) Sammalkorpi, M.; Krasheninnikov, A.; Kuronen, A.; Nordlund, K.; Kaski, K. *Phys. Rev. B* **2004**, *70*, 245416.
(14) Zhang, S.; Mielke, S. L.; Khare, R.; Troya, D.; Ruoff, R. S.; Schatz, G. C.; Belytschko, T. *Phys. Rev. B* **2005**, *71*, 115403.
(15) Basiuk, V. A.; Kobayashi, K.; Kaneko, T.; Negishi, Y.; Basiuk, E. V.; Saniger-Blesa, J.-M. *Nano Lett.* **2002**, *2*, 789.
(16) Popov, M.; Kyotani, M.; Nemanich, R. J.; Koga, Y. *Phys. Rev. B* **2002**, *65*, 033408.
(17) Khabashesku, V. N.; Gu, Z.; Brinson, B.; Zimmerman, J. L.; Margrave, J. L.; Davydov, V. A.; Kashevarova, L. S.; Rakhmanina, A. V. *J. Phys. Chem.* **2002**, *106*, 11155.
(18) Kawasaki, S.; Hara, T.; Yokomae, T.; Okino, F.; Touhara, H.; Kataura, H.; Watanuki, T.; Ohishi, Y. *Chem. Phys. Lett.* **2006**, *418*, 260.
(19) Braga, S. F.; Galvão, D. S. *Chem. Phys. Lett.* **2006**, *419*, 394.
(20) Salonen, E.; Krasheninnikov, A. V.; Nordlund, K. *Nucl. Instrum. Methods B* **2002**, *193*, 603
(21) Krasheninnikov, A. V.; Nordlund, K.; Keinonen, J. *Phys. Rev. B* **2002**, *65*, 165423.
(22) Krasheninnikov, A. V.; Nordlund, K. *Nucl. Instrum. Methods B* **2004**, *216*, 355.
(23) Ma, J.; Huo, D. Y.; Cui, F. Z. *Nucl. Instrum. Methods B* **2005**, *239*, 159.
(24) Pregler, S. K.; Sinnott, S. B. *Phys. Rev. B* **2006**, *73*, 224106.
(25) Kotakoski, J.; Krasheninnikov, A. V.; Nordlund, K. *Nucl. Instrum. Methods B* **2005**, *220*, 810.
(26) Kotakoski, J.; Krasheninnikov, A. V.; Ma, Y.; Foster, A. A.; Nordlund, K.; Nieminem, R. M. *Phys. Rev. B* **2005**, *71*, 205408.
(27) Chan, S.-P.; Chen, G.; Gong, X. G.; Liu, Z.-F. *Phys. Rev. Lett.* **2001**, *87*, 205502.
(28) Zhao, J.; Buldun, A.; Han, J.; Lu, J. P. *Nanotechnology* **2002**, *13*, 195.
(29) Fagan, S. B.; Fazzio, A.; Mota, R. *Nanotechnology* **2006**, *17*, 1154.
(30) Bachtold, A.; Strunk, C.; Salvetat, J.-P.; Bonard, J.-M.; Forró, L.; Nussbaumer, T.; Schönenberger, C. *Nature* **1999**, *397*, 673.
(31) Gómez-Navarro, C.; de Pablo, P. J.; Gómez-Herrero, J.; Biel, B.; Garcia-Vidal, F. J.; Rubio, A.; Flores, F. *Nat. Mater.* **2005**, *4*, 534.
(32) Tersoff, J. *Phys. Rev. Lett.* **1988**, *61*, 2879.
(33) Ziegler, J.; Biersack, J. P.; Littmark, U. *The stopping and range of ions in solids*; Pergamon: New York, 1985; 35.
(34) Moura, C. S.; Amaral L. *J. Phys. Chem. B* **2005**, *109*, 13515.
(35) Moura, C. S.; Amaral L. Submitted to publication.
(36) Andersen, H. C. *J. Chem. Phys.* **1980**, *72*, 2384.